JACS
JOURNAL OF THE AMERICAN CHEMICAL SOCIETY

Article

pubs.acs.org/JACS

Intracellular Guest Exchange between Dynamic Supramolecular Hosts

Subramani Swaminathan,[†] Colin Fowley,[‡] Bridgeen McCaughan,[‡] Janet Cusido,[†] John F. Callan,*[,‡] and Françisco M. Raymo*[,†]

[†]Laboratory for Molecular Photonics, Department of Chemistry, University of Miami, 1301 Memorial Drive, Coral Gables, Florida 33146-0431, United States

[‡]School of Pharmacy and Pharmaceutical Sciences, University of Ulster, Coleraine, BT52 1SA Northern Ireland, United Kingdom

Supporting Information

ABSTRACT: Decyl and oligo(ethylene glycol) chains were appended to the same poly(methacrylate) backbone to generate an amphiphilic polymer with a ratio between hydrophobic and hydrophilic segments of 2.5. At concentrations greater than 10 μg mL^{-1} in neutral buffer, multiple copies of this particular macromolecule assemble into nanoparticles with a hydrodynamic diameter of 15 nm. In the process of assembling, these nanoparticles can capture anthracene donors and borondipyrromethene acceptors within their hydrophobic interior and permit the transfer of excitation energy with an efficiency of 95%. Energy transfer is observed also if nanocarriers containing exclusively the donors are mixed with nanoparticles preloaded separately with the acceptors in aqueous media. The two sets of supramolecular assemblies exchange their guests with fast kinetics upon mixing to co-localize complementary chromophores within the same nanostructured container and enable energy transfer. After guest exchange, the nanoparticles can cross the membrane of cervical cancer cells and bring the co-entrapped donors and acceptors within the intracellular environment. Alternatively, intracellular energy transfer is also established after sequential cell incubation with nanoparticles containing the donors first and then with nanocarriers preloaded with the acceptors or *vice versa*. Under these conditions, the nanoparticles exchange their cargo only after internalization and allow energy transfer exclusively within the cell interior. Thus, the dynamic character of such supramolecular containers offers the opportunity to transport independently complementary species inside cells and permit their interaction only within the intracellular space.

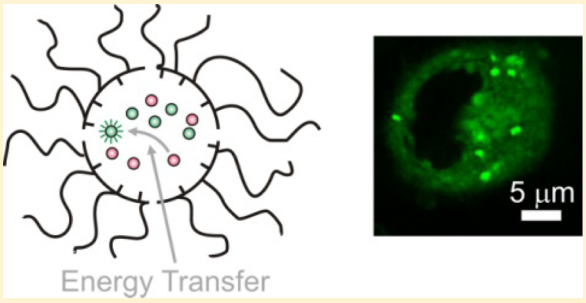

INTRODUCTION

Supramolecular constructs assemble spontaneously from complementary building blocks under the influence of noncovalent bonds.[1] A subtle balance of steric and electronic factors dictates the interaction mode and number of their constituent components to define ultimately the overall dimensions and shapes of the final assemblies. In addition, the moderate enthalpic contributions of noncovalent contacts, relative to their covalent counterparts, ensure reversibility and impose dynamic character on supramolecular systems. Indeed, the association and disassociation of noncovalent synthons can occur continuously on relatively short time scales, under appropriate experimental conditions, to exchange rapidly the building blocks of independent supramolecular assemblies. Thus, the reversibility of noncovalent interactions offers the attractive opportunity to engineer the controlled scrambling of simple molecular components within complex chemical ensembles that is difficult to replicate with the sole assistance of covalent bonds.[2−6]

Nanoparticles of amphiphilic polymers are a remarkable example of self-assembling supramolecular systems.[7−13] The hydrophilic and hydrophobic segments, integrated covalently within their macromolecular components, are responsible for their spontaneous assembly in aqueous environments. Specifically, noncovalent contacts bring the hydrophobic domains of distinct amphiphilic macromolecules together in order to minimize their direct exposure to water. In turn, the hydrophilic counterparts within the same macromolecular building blocks protrude into bulk solution and ensure optimal solvation of the overall supramolecular constructs. In the process of assembling, these polymer nanoparticles can also capture multiple hydrophobic molecules and retain them in their hydrophobic interiors. In fact, the encapsulation of molecular guests within these supramolecular hosts ensures, once again, minimal exposure of the entrapped species to water. As a result, such polymer nanoparticles can be valuable vehicles to transfer molecules, which would otherwise be insoluble in water, across aqueous media. Indeed, these particular supramolecular nanocarriers can transport drugs through the bloodstream as well as penetrate the membrane of living cells and deliver their cargo intracellularly.[14−23]

Received: January 10, 2014
Published: May 9, 2014

   dx.doi.org/10.1021/ja500285p | J. Am. Chem. Soc. 2014, 136, 7907−7913

The ability of self-assembling nanoparticles of amphiphilic polymers to capture hydrophobic compounds can be exploited to entrap multiple chromophores within the same supramolecular container and impose photoresponsive character on the resulting construct.[24] In particular, this supramolecular strategy offers the opportunity to constrain complementary donors and acceptors in close proximity and promote the transfer of excitation energy from the former components to the latter. Such operating principles are especially valuable to engineer fluorescent materials with emissive behavior that would otherwise be impossible to achieve with their separate chromophoric components.[25−29] In addition, they also make it possible to assess the stability of the polymer nanocarriers under a broad range of experimental conditions.[30−41] Indeed, only if the supramolecular containers retain their integrity can the complementary donors and acceptors remain sufficiently close to each other and transfer energy efficiently upon excitation. Furthermore, the occurrence of energy transfer can also signal the exchange of molecular guests between independent nanostructured hosts.[30,33,34a,c,37] In fact, these dynamic supramolecular assemblies can barter their macromolecular components and trade their entrapped cargo on relatively short time scales, under appropriate experimental conditions.

The unique properties of self-assembling nanoparticles of amphiphilic polymers suggest that strategies to bring complementary molecules in close proximity exclusively within the intracellular environment, and only then enforce their mutual interaction, can be implemented with the aid of such dynamic supramolecular containers. In principle, distinct hydrophobic guests can be transported sequentially across the membrane of the very same cell with independent nanoparticle hosts. Once internalized, the nanocarriers can exchange their components and, only then, permit the chemical reaction or photophysical interaction of their complementary cargos. For example, the intracellular conversion of a pro-drug into a drug, under the influence of an appropriate activator, can be envisaged on the basis of this general mechanism. This article demonstrates with a representative example of intracellular energy transfer that such operating principles to enforce interactions between complementary species exclusively inside living cells can, indeed, be implemented experimentally.

RESULTS AND DISCUSSION

Energy Transfer between Guests Entrapped within Dynamic Supramolecular Hosts. The pronounced hydrophobic character of **1** and **2** (Figure 1) translates into negligible aqueous solubility. In the presence of **3**, however, both molecules dissolve readily in neutral phosphate buffered saline (PBS). Indeed, the hydrophilic oligo(ethylene glycol) and hydrophobic decyl chains of this particular amphiphilic polymer ensure the spontaneous assembly of nanocarriers capable of capturing either **1** or **2** in their interiors.[42] Consistently, dynamic light scattering measurements confirm the formation of particles with nanoscaled dimensions in both instances. Specifically, these analyses indicate that the hydrodynamic diameter of the nanocarriers is ca. 15 nm and that this value does not change significantly with the nature of the encapsulated guest and its amount relative to the polymer host (***a*** and ***b*** in Supplementary Figure S1).[43]

The absorption spectra (***a*** and ***b*** in Figure 1) of nanoparticles of **3**, loaded with either **1** or **2**, in PBS reveal the characteristic bands of the anthracene or borondipyrromethene (BODIPY)

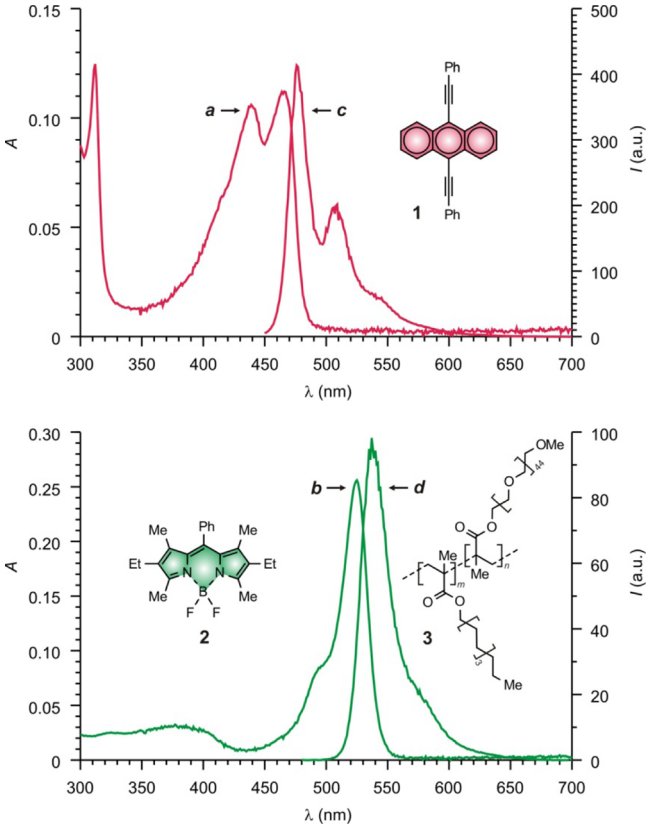

Figure 1. Absorption (***a*** and ***b***) and emission (***c*** and ***d***) spectra of nanoparticles of **3** (500 μg mL^{-1}), loaded with either **1** (***a*** and ***c***, 2 μg mL^{-1}, λ_{Ex} = 440 nm) or **2** (***b*** and ***d***, 2 μg mL^{-1}, λ_{Ex} = 470 nm), in PBS at 25 °C.

chromophores, respectively. These bands closely resemble those (***a*−*d*** in Supplementary Figure S2) observed for **1** and **2** in tetrahydrofuran (THF) but cannot be detected when these molecules are treated with PBS in the absence of **3**. Thus, the self-assembling nanocarriers are responsible for transferring significant amounts of **1** and **2** in the aqueous medium, and in doing so, these supramolecular containers provide an environment to the encapsulated chromophores similar to that experienced by both in THF. Furthermore, the absorption bands of the entrapped guests remain unchanged for hours, upon storage of the PBS dispersions in the dark at ambient temperature, indicating that the nanoparticles retain their integrity under these experimental conditions.

The corresponding emission spectra (***c*** and ***d*** in Figure 1) also show the characteristic bands of the anthracene and BODIPY chromophores, enclosed within the nanocarriers, and do not change even after several hours of storage in the dark. Once again, these bands closely resemble those (***e*−*h*** in Supplementary Figure S2) observed for **1** and **2** in THF. The fluorescence quantum yield, however, decreases by ca. 30% in both instances with the encapsulation of the emissive guests in the nanostructured hosts. Specifically, this parameter changes from 0.85 to 0.58 for **1** and from 0.72 to 0.51 for **2** with the transition from THF solution to the interior of the nanocarriers dispersed in PBS. Thus, the entrapment of these fluorophores within the nanocarriers has negligible influence on the emission wavelengths but a moderate depressive effect on the efficiency of their radiative deactivation. Furthermore, the negligible solubility of **1** and **2** in aqueous media prevents the detection of

dx.doi.org/10.1021/ja500285p | J. Am. Chem. Soc. 2014, 136, 7907−7913

their emission in the absence of **3**. Specifically, plots (***a*** and ***b*** in Supplementary Figure S3) of their emission intensities, measured in PBS dispersions containing increasing amounts of **3**, indicate that the polymer concentration must be greater than 10 μg mL^{-1} to encourage the transfer of significant amounts of either one of the two fluorophores in aqueous environments.[43]

The emission band (***c*** in Figure 1) of **1** is positioned within the same spectral window of the absorption band (***b*** in Figure 1) of **2**. Their overlap integral is 9.1×10^{-14} M^{-1} cm^3, and the corresponding Förster distance is 47 Å.[44] These values suggest that the co-entrapment of both chromophores within the same nanocarrier can result in the efficient transfer of energy from **1** to **2** upon excitation of the former. Indeed, a comparison of the emission spectra (***a*** and ***b*** in Figure 2) of nanoparticles

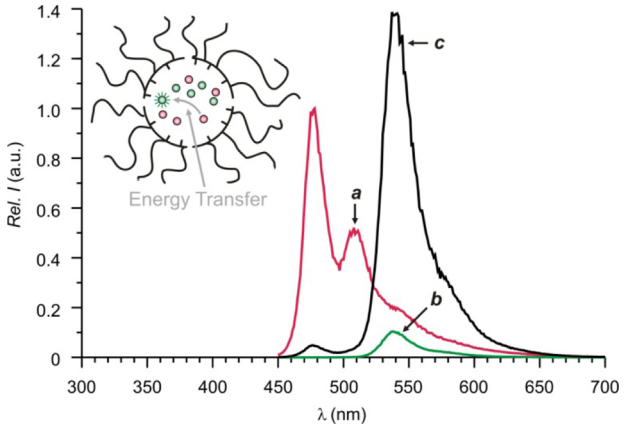

Figure 2. Emission spectra (λ_{Ex} = 430 nm) of nanoparticles of **3** (500 μg mL^{-1}), loaded with **1** (***a***, 5 μg mL^{-1}), **2** (***b***, 5 μg mL^{-1}), or both (***c***), in PBS at 25 °C.

containing exclusively either **1** or **2** to that (***c*** in Figure 2) of nanocarriers loaded with both clearly confirms the occurrence of energy transfer. Specifically, the emission intensity of the anthracene donors decreases significantly and that of the BODIPY acceptors increases dramatically when both species are co-encapsulated in the same supramolecular container. The ratio between the emission intensity of the anthracene donors in the presence of the BODIPY acceptors and that in their absence indicates the efficiency of energy transfer to be 95%.

The nanoparticles doped with both chromophores were prepared by co-dissolving **1**, **2**, and **3** in chloroform and, after the evaporation of the organic solvent, dispersing the residue in PBS. This experimental protocol ensures the entrapment of both guests in the same supramolecular container and enables energy transfer. However, the very same result is also achieved if a PBS dispersion of nanoparticles loaded exclusively with **1** is mixed with one of nanocarriers doped independently with **2**. Upon mixing, these dynamic supramolecular assemblies exchange their components, and eventually, nanostructured containers with the two distinct chromophores in their interior are produced. Indeed, the emission spectrum (***a*** in Figure 3) recorded immediately after mixing closely resembles that (***c*** in Figure 2) of nanoparticle preloaded with both guests. Once again, the emission of the anthracene donors is almost completely suppressed with a concomitant enhancement in the fluorescence of the BODIPY acceptors. Furthermore, the spectrum of the mixture does not change with time, indicating that the components of these supramolecular assemblies

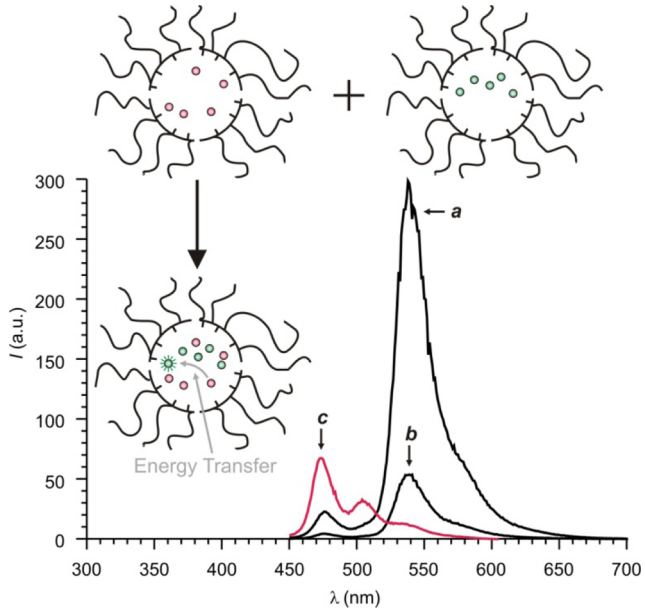

Figure 3. Emission spectra (λ_{Ex} = 430 nm) recorded at 25 °C after mixing identical volumes of two PBS dispersions of nanoparticles of **3** (500 μg mL^{-1}), loaded with **1** (5 μg mL^{-1}) or **2** (5 μg mL^{-1}), respectively, before (***a***) and after 10-fold dilution with either PBS (***b***) or THF (***c***).

exchange with fast kinetics to establish thermodynamic equilibrium essentially upon mixing, under the experimental conditions employed. In principle, two possible pathways can be envisaged for the rapid exchange of the chromophoric guests between independent nanoparticles. Specifically, a fraction of the encapsulated molecules can escape from one nanostructured container into bulk solution and then be captured by another. Alternatively, the collision of independent nanoparticles might result in the exchange of their macromolecular components together with part of their cargo. The former mechanism requires the hydrophobic guests to leak out into the aqueous environment, while the latter can occur with minimal exposure of the guests to water. The lack of any significant aqueous solubility for both **1** and **2** (Supplementary Figure S3) suggests that, presumably, the second pathway is mostly responsible for guest exchange.

For the nanoparticles preloaded with both donors and acceptors as well as for those obtained after guest exchange, the energy-transfer efficiency remains unaltered even after a 10-fold dilution with PBS. In fact, the resulting emission spectra (e.g., ***b*** in Figure 3) scale linearly with dilution. Instead, the transfer of energy is completely suppressed if the nanoparticles are diluted 10-fold with THF. This organic solvent dismembers the supramolecular containers, separates the donors from the acceptors, and prevents energy transfer. Consistently, the corresponding emission spectra (e.g., ***c*** in Figure 3) show predominantly the donor emission. Thus, these observations demonstrate that the co-encapsulation of the complementary donors and acceptors within the same nanoparticles is essential for efficient energy transfer to occur and that independent nanocarriers exchange rapidly their cargo.

Intracellular Cargo Exchange between Dynamic Nanocarriers. The incubation of cervical cancer (HeLa) cells with nanoparticles of **3**, loaded with either **1** or **2**, results in the internalization of the supramolecular containers and their cargo. Fluorescence measurements (***a*–*d*** in Supplementary

dx.doi.org/10.1021/ja500285p | J. Am. Chem. Soc. 2014, 136, 7907−7913

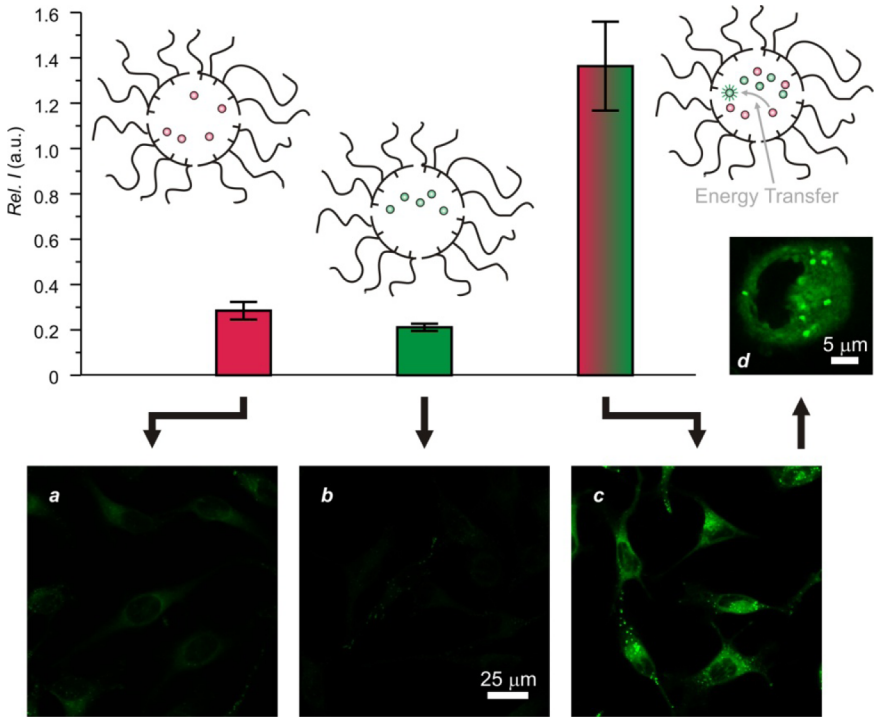

Figure 4. Fluorescence images (λ_{Ex} = 458 nm, λ_{Em} = 540−640 nm) of HeLa cells recorded after incubation with PBS dispersions of nanoparticles of **3** (125 μg mL^{-1}), loaded with either **1** (***a***, 1.25 μg mL^{-1}) or **2** (***b***, 1.25 μg mL^{-1}) or after incubation with a mixture (1:1, v/v) of both dispersions (***c*** and ***d***) for 3 h and washing together with the corresponding emission intensities measured along lines drawn across individual cells and reported relative to that of an indocyanine green standard (50 μM, λ_{Ex} = 628 nm, λ_{Em} = 780−800 nm) added 30 min prior to termination of incubation.

Figure S4), performed with a plate reader after washing the incubated cells, reveal the characteristic emission of the internalized fluorophores in both instances. Consistently, the acquisition of fluorescence images (***a*** and ***b*** in Figure 4) of cells treated with nanocarriers containing either **1** or **2** show emission predominantly in the intracellular space. Both images were recorded by exciting the fluorophores at 458 nm, where the absorbance of **1** is significant and that of **2** is negligible (***a*** and ***b*** in Figure 1), and collecting their fluorescence between 540 and 640 nm, where the emission of **1** is negligible and that of **2** is significant (***c*** and ***d*** in Figure 1). As a result of this choice of wavelengths, the detected intracellular fluorescence is relatively weak in both instances. By contrast, an image (***c*** and ***d*** in Figure 4) of cells incubated with a mixture of two sets of nanoparticles loaded separately with **1** and **2** clearly reveals intense fluorescence within the intracellular space, under otherwise identical experimental conditions.[45] The obvious increase in emission intensity indicates that energy is transferred between the internalized chromophores. Indeed, the predominant excitation of the anthracene donors at 458 nm is followed by the transfer of energy to the BODIPY acceptors with concomitant emission between 540 and 640 nm (cf., ***a*** in Figure 3). Consistently, the emission intensities (bars in Figure 4) measured along lines drawn across cells in the three images indicate 5- or 7-fold fluorescence enhancements for the cells incubated with both chromophores, relative to those treated with only **1** or **2** respectively.[46] In addition, the localization of the nanocarriers within the intracellular space is further confirmed by the fluorescence evolution in the vertical direction evident in a stack of images (***a***−***e*** in Supplementary Figure S9) recorded by displacing stepwise the focal plane along the optic axis. Moreover, the intracellular localization of the supramolecular assemblies is in full agreement with published data on similar polymer nanoparticles.[47,48] These literature precedents suggest that the cellular uptake of the nanocarriers is mostly a consequence of clathrin- and caveolae-mediated endocytosis and, ultimately, results in their predominant localization within endosomes and lysosomes. In order to support this hypothesis, cells were incubated with two sets of nanoparticles, loaded separately with **1** and **2**, and either chlorpromazine or genistein. These two compounds are known to inhibit clathrin- or caveolae-mediated endocytosis, respectively.[49] Indeed, their presence reduced the intracellular fluorescence to 59% or 90%, respectively (***a***−***c*** Supplementary Figure S10). These observations indicate that clathrin-mediated endocytosis is predominantly responsible for the cellular internalization of the nanoparticles.

The intracellular transfer of energy, evident in the corresponding fluorescence image (***c*** and ***d*** in Figure 4), is achieved by allowing the nanocarriers to exchange their guests in the extracellular space and then transport mixtures of co-encapsulated donors and acceptor to the cytosol. Alternatively, the complementary chromophoric species can be delivered sequentially to the cytosol by incubating the very same cells with nanoparticles containing the acceptors first and then nanocarriers loaded with the donors or *vice versa*. Under these conditions, the two sets of internalized supramolecular hosts can exchange their guests and enable energy transfer. In particular, comparison of the emission intensities recorded at 540 nm, where the fluorescence of the BODIPY chromophores is centered (***d*** in Figure 1), for cells before (***a*** in Figure 5) and after incubation with nanoparticles containing **2** (***b*** in Figure 5) confirms the intracellular loading of the fluorescent species. These measurements were performed with a plate reader operating at an excitation wavelength of 430 nm, where the absorbance of the BODIPY acceptors is negligible (***b*** in Figure

dx.doi.org/10.1021/ja500285p | *J. Am. Chem. Soc.* 2014, 136, 7907−7913

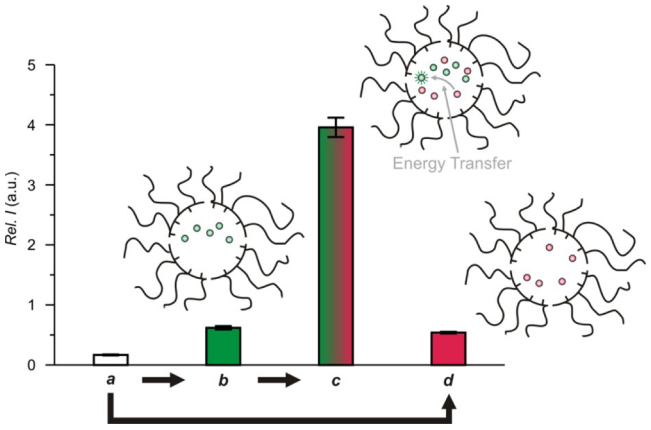

Figure 5. Emission intensities (λ_{Ex} = 430 nm, λ_{Em} = 540 nm), reported relative to that of an indocyanine green standard (50 μM, λ_{Ex} = 730 nm, λ_{Em} = 780 nm) added 30 min prior to termination of incubation, recorded with a plate reader before (***a***) and after incubation of HeLa cells with a PBS dispersion of nanoparticles of **3** (125 μg mL^{-1}), containing **2** (1.25 μg mL^{-1}), for 3 h and washing (***b***) and subsequent incubation with a PBS dispersion of nanocarriers of **3** (125 μg mL^{-1}), containing **1** (1.25 μg mL^{-1}), for a further 3 h and washing (***c***) or after incubation with the same dispersion of nanoparticles, containing **1**, for 3 h and washing (***d***).

1) but that of the anthracene donors is significant (***a*** in Figure 1). As a result, the further incubation of the very same cells with nanoparticles containing **1** translates into a dramatic fluorescence enhancement (***c*** in Figure 5). Thus, the sequential treatment of the cells with the two sets of nanocarriers ultimately positions donors and acceptors in close proximity within the intracellular space and permits the efficient transfer of energy between them. In agreement with this interpretation, the emission intensity (***d*** in Figure 5) measured for cells incubated only with nanoparticles containing **1**, under otherwise identical conditions, is approximately one-third of that detected after sequential incubation. Therefore, the presence of both chromophores is essential for a pronounced fluorescence increase to be observed. Furthermore, intracellular energy transfer is established also if the order of the two incubation steps is inverted. In fact, images (***a*** and ***b*** in Figure 6) of cells treated with one set of nanoparticles first and then the other or *vice versa* reveal essentially the same emission intensity. In both instances, the dynamic character of the supramolecular hosts permits the co-localization of the complementary guests and enables energy transfer in the intracellular space.

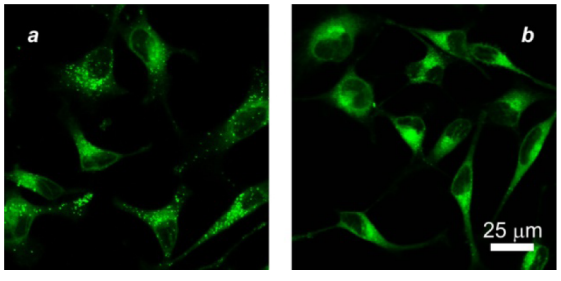

Figure 6. Fluorescence images (λ_{Ex} = 458 nm, λ_{Em} = 540−640 nm) of HeLa cells recorded after incubation with a PBS dispersion of nanoparticles of **3** (125 μg mL^{-1}), containing **2** (1.25 μg mL^{-1}), for 3 h, washing and subsequent incubation with a PBS dispersion of nanocarriers of **3** (125 μg mL^{-1}), containing **1** (1.25 μg mL^{-1}), and washing (***a***) or after the same treatment but inverting the order of addition of the two components (***b***).

CONCLUSIONS

Self-assembling nanoparticles of amphiphilic polymers can capture mixtures of complementary energy donors and acceptors in their hydrophobic interiors. The spectral overlap of the encapsulated chromophores and their close proximity within the supramolecular containers ensure energy transfer with essentially unitary efficiency. Furthermore, the dynamic character of these self-assembling nanocarriers translates into the rapid equilibration of their constituent components at ambient temperature in neutral buffer. As a result, pairs of nanoparticles, loaded independently with donors and acceptors, respectively, can exchange their cargo upon mixing and enable energy transfer. In addition, the nanocarriers can cross the membrane of living cells and transport their fluorescent cargo to the intracellular space. In fact, intracellular energy transfer is clearly detected when the cells are incubated with two sets of self-assembling nanoparticles preloaded independently with acceptors and donors. Under these conditions, the dynamic supramolecular hosts exchange their guests and then shuttle co-encapsulated donors and acceptors to the intracellular space. Alternatively, two consecutive incubation steps can be exploited to transport the complementary chromophoric components to the cytosol in sequence. After the second step, the internalized nanoparticles exchange their complementary guests in the cytosol to bring them in close proximity and allow energy transfer. Thus, the dynamic character of such self-assembling nanocarriers, coupled to their ability to cross the cell membrane, translates into an attractive supramolecular strategy to transport complementary species inside cells and allow their mutual interactions exclusively within the intracellular space.

EXPERIMENTAL PROCEDURES

Materials and Methods. Chemicals were purchased from commercial sources and used as received with the exception of THF, which was distilled over sodium and benzophenone. Compounds **2** and **3** were prepared according to literature procedures.[28,50] Dynamic light scattering measurements were performed with a Malvern ZEN1600 apparatus, and ^{1}H nuclear magnetic resonance spectra were recorded with a Bruker Avance 400 spectrometer. Absorption spectra were recorded with a Varian Cary 100 Bio spectrometer, using quartz cells with a path length of 1.0 cm. Emission spectra were recorded with a Varian Cary Eclipse spectrometer in aerated solutions. Fluorescence quantum yields were measured with a fluorescein standard, following a literature protocol.[51] Plate readings were performed with a Flex station at 540 nm, using an excitation wavelength of either 430 or 458 nm. The emission intensities of the bars in Supplementary Figures S4 and S10 are absolute values. Those in Figure 5 are reported relative to that of an indocyanine green standard. The fluorescence of the standard was recorded at 780 nm with an excitation at 730 nm. Fluorescence images were recorded with a Leica SP5 confocal laser-scanning multiphoton microscope, equipped with an incubator maintained at 37 °C in O_2/CO_2/air (20:5:75, v/v/v). The emission intensity was recorded between 540 and 640 nm, using an excitation wavelength of 458 nm, and is reported relative to that of an indocyanine green standard in the corresponding bar charts. Specifically, the emission intensities of fluorescent guests and standard were measured along four lines drawn across cells and the ratio between the two is quoted. The fluorescence of the standard was recorded between 780 and 800 nm with an excitation wavelength of 628 nm. The fluorescence of Hoechst 33342

dx.doi.org/10.1021/ja500285p | *J. Am. Chem. Soc.* 2014, 136, 7907−7913

was recorded between 420 and 450 nm with two-photon excitation at 720 nm.

Polymer Nanoparticles. A $CHCl_3$ solution of **3** (2.5 mg mL^{-1}, 200 μL) was added to various aliquots (0–50 μL) of stock solutions of **1**, **2**, or both compounds in $CHCl_3$. The concentration of each guest in the stock solutions was 0.1 mg mL^{-1}. The resulting mixtures were heated at 40 °C in open vials. After the evaporation of the solvent, the residues were purged with air and dispersed in PBS (1.0 mL, pH = 7.0). After vigorous shaking, the dispersions were filtered, and the filtrates were used for spectroscopic and imaging experiments without further purification.

Cells. HeLa cells were cultured in Dulbecco's modified Eagle's media supplemented with fetal bovine serum (10%, v/v), penicillin (200 U mL^{-1}), streptomycin (200 μg mL^{-1}), and nonessential amino acids (0.1 mM) and incubated at 37 °C in O_2/CO_2/air (20:5:75, v/v/v). The cells were seeded in 384-well glass-bottom plates at a density of 5 × 104 cells mL^{-1} and incubated overnight at 37 °C in O_2/CO_2/air (20:5:75, v/v/v). The cultured cells were incubated further with PBS dispersions (25%, v/v) of nanoparticles of **3** (125 μg mL^{-1}) loaded with either **1** (1.25 μg mL^{-1}) or **2** (1.25 μg mL^{-1}) or with a mixture (1:1, v/v) of both dispersions for 3 h and then washed three times with PBS (80 μL). Alternatively, they were incubated with nanoparticles containing either one of the two guests for 3 h, washed three times, incubated with nanoparticles loaded with the other for a further 3 h, and washed three more times. Internal standard indocyanine green (50 μM) was added to all wells 30 min prior to termination of incubation with nanoparticles. Inhibition experiments were performed by adding either chlorpromazine (30 μM) or genistein (150 μM) to the cells 30 min prior to incubation with nanoparticles preloaded with a mixture of **1** and **2**. Nuclear staining experiments were performed by adding Hoechst 33342 (25 μM) to the cells 30 min prior to termination of incubation with nanoparticles.

■ ASSOCIATED CONTENT

Ⓢ Supporting Information

Dynamic light scattering measurements; absorption and emission spectra in THF and PBS; dependence of the emission intensity on the polymer concentration; intracellular fluorescence measurements; fluorescence images with nuclear staining; fluorescence images with internal standard; fluorescence images with vertical displacement of the focal plane; intracellular fluorescence measurements in the presence of endocytosis inhibitors. This material is available free of charge via the Internet at http://pubs.acs.org.

■ AUTHOR INFORMATION

Corresponding Authors

J.Callan@ulster.ac.uk
fraymo@miami.edu

Notes

The authors declare no competing financial interest.

■ ACKNOWLEDGMENTS

JFC acknowledges support from Norbrook Laboratories Ltd. FMR acknowledges support from the National Science Foundation (CAREER Award CHE-0237578, CHE-0749840 and CHE-1049860).

■ REFERENCES

(1) (a) Lehn, J.-M. *Proc. Natl. Acad. Sci. U.S.A.* **2002**, *99*, 4763–4768. (b) Lehn, J.-M. *Science* **2002**, *295*, 2400–2403.

(2) (a) Lehn, J.-M. *Chem.—Eur. J.* **1999**, *5*, 2455–2463. (b) Lehn, J.-M. *Chem.—Eur. J.* **2000**, *12*, 2097–2102. (c) Lehn, J.-M. *Chem. Soc. Rev.* **2007**, *36*, 151–160. (d) Lehn, J.-M. *Top. Curr. Chem.* **2012**, *322*, 1–32. (e) Lehn, J.-M. *Angew. Chem., Int. Ed.* **2013**, *52*, 2836–2850.

(3) (a) Rowan, S. J.; Cantrill, S. J.; Cousins, G. R. L.; Sanders, J. K. M.; Stoddart, J. F. *Angew. Chem., Int. Ed.* **2002**, *41*, 899–958. (b) Belowich, M.; Stoddart, J. F. *Chem. Soc. Rev.* **2012**, *41*, 2003–2024. (c) Stoddart, J. F. *Angew. Chem., Int. Ed.* **2012**, *51*, 12902–12903.

(4) Cheeseman, J. D.; Corbett, A. D.; Gleason, J. L.; Kazlauskas, R. J. *Chem.—Eur. J.* **2005**, *11*, 1708–1716.

(5) (a) Corbett, P. T.; Leclaire, J.; Vial, L.; West, K. R.; Wietor, J.-L.; Sanders, J. K. M.; Otto, S. *Chem. Rev.* **2006**, *106*, 3652–3711. (b) Cougnon, F. B. L.; Sanders, J. K. M. *Acc. Chem. Res.* **2012**, *45*, 2211–2221.

(6) Ladame, S. *Org. Biomol. Chem.* **2008**, *6*, 219–226.

(7) (a) Halperin, A.; Tirrell, M.; Lodge, T. P. *Adv. Polym. Sci.* **1992**, *100*, 31–71. (b) Lodge, T. P. *Macromol. Chem. Phys.* **2003**, *204*, 265–273. (c) Moughton, A. O.; Hillmyer, M. A.; Lodge, T. P. *Macromolecules* **2012**, *45*, 2–19.

(8) (a) Moffitt, M.; Khougaz, K.; Eisenberg, A. *Acc. Chem. Res.* **1996**, *29*, 95–102. (b) Cameron, N. S.; Corbierre, K. M.; Eisenberg, A. *Can. J. Chem.* **1999**, *77*, 1311–1326.

(9) Webber, S. E. *J. Phys. Chem. B* **1998**, *102*, 2618–2626.

(10) Riess, G. *Prog. Polym. Sci.* **2003**, *28*, 1107–1170.

(11) Okhapkin, I. M.; Makhaeva, E. E.; Khokhlov, A. R. *Adv. Polym. Sci.* **2006**, *195*, 177–210.

(12) Kale, T. S.; Klaikherd, A.; Popere, B.; Thayumanavan, S. *Langmuir* **2009**, *25*, 9660–9670.

(13) Owen, S. C.; Chan, D. P. Y.; Shoichet, M. S. *Nano Today* **2012**, *7*, 53–65.

(14) Bader, H.; Ringsdorf, H.; Schmidt, B. *Angew. Makromol. Chem.* **1984**, *123*, 457–485.

(15) Kataoka, K.; Kwon, G. S.; Yokoyama, M.; Okano, T.; Sakurai, Y. *J. Controlled Release* **1993**, *24*, 119–132.

(16) Jones, M.-C.; Leroux, J.-C. *Eur. J. Pharm. Biopharm.* **1999**, *48*, 101–111.

(17) Torchilin, V. P. *J. Controlled Release* **2001**, *73*, 137–172.

(18) Adams, M. L.; Lavasanifar, A.; Kwon, G. S. *J. Pharm. Sci.* **2003**, *92*, 1343–1355.

(19) Husseini, A. G.; Pitt, W. G. *Adv. Drug Delivery Rev.* **2008**, *60*, 1137–1152.

(20) Mondon, K.; Gurny, R.; M?ller, M. *Chimia* **2008**, *62*, 832–840.

(21) Park, J. H.; Lee, S.; Kim, J. H.; Park, K.; Kim, K.; Kwon, I. C. *Prog. Polym. Sci.* **2008**, *33*, 113–137.

(22) Kim, S.; Shi, Y.; Kim, J. Y.; Park, K.; Cheng, J.-X. *Expert Opin. Drug Delivery* **2010**, *7*, 49–62.

(23) Nicolas, J.; Mura, S.; Brambilla, D.; Mackiewicz, N.; Couvreur, P. *Chem. Soc. Rev.* **2013**, *42*, 1147–1235.

(24) Swaminathan, S.; Garcia-Amorós, J.; Fraix, A.; Kandoth, N.; Sortino, S.; Raymo, F. M. *Chem. Soc. Rev.* **2014**, DOI: 10.1039/C3CS60324E.

(25) (a) Yoo, S. I.; An, S. J.; Choi, G. H.; Kim, K. S.; Yi, G.-C.; Zin, W.-C.; Jung, J. C.; Sohn, B.-H. *Adv. Mater.* **2007**, *19*, 1594–1596. (b) Yoo, S. I.; Lee, J.-H.; Sohn, B.-H.; Eom, I.; Joo, T.; An, S. J.; Yi, G.-C. *Adv. Funct. Mater.* **2008**, *18*, 2984–2989.

(26) Wu, W.-C.; Chen, C.-Y.; Tian, Y.; Jang, S.-H.; Hong, Y.; Liu, Y.; Hu, R.; Tang, B. Z.; Lee, Y.-T.; Chen, C.-T.; Chen, W.-C.; Jen, A. K.-Y. *Adv. Funct. Mater.* **2010**, *29*, 1413–1423.

(27) Wang, R.; Peng, J.; Qiu, F.; Yang, Y. *Chem. Commun.* **2011**, *47*, 2787–2789.

(28) Yildiz, I.; Impellizzeri, S.; Deniz, E.; McCaughan, B.; Callan, J. F.; Raymo, F. M. *J. Am. Chem. Soc.* **2011**, *133*, 871–879.

(29) Wagh, A.; Qian, S. Y.; Law, B. *Bioconjugate Chem.* **2012**, *23*, 981–992.

(30) (a) Cao, T.; Munk, P.; Ramireddy, C.; Tuzar, Z.; Webber, S. E. *Macromolecules* **1991**, *24*, 6300–6305. (b) Stepanek, M.; Krijtova, K.; Prochazka, K.; Teng, Y.; Webber, S. E.; Munk, P. *Acta Polym.* **1998**, *49*, 96–102.

(31) Hu, Y.; Kramer, M. C.; Boudreaux, C. J.; McCormick, C. L. *Macromolecules* **1995**, *28*, 7100–7106.

(32) (a) Chen, H.; Kim, S.; He, W.; Wang, H.; Low, P. S.; Park, K.; Cheng, J. X. *Langmuir* **2008**, *24*, 5213–5217. (b) Chen, H. T.; Kim, S. W.; Li, L.; Wang, S. Y.; Park, K.; Cheng, J. X. *Proc. Natl. Acad. Sci.*

U.S.A. **2008**, *105*, 6596−6601. (c) Lee, S.-Y.; Tyler, J. Y.; Kim, S.; Park, K.; Cheng, J.-X. *Mol. Pharmaceutics* **2013**, *10*, 3497−3506.
(33) Njikang, G. N.; Gauthier, M.; Li, J. M. *Polymer* **2008**, *49*, 5474−5481.
(34) (a) Jiwpanich, S.; Ryu, J. H.; Bickerton, S.; Thayumanavan, S. *J. Am. Chem. Soc.* **2010**, *132*, 10683−10685. (b) Ryu, J. H.; Chacko, R. T.; Jiwpanich, S.; Bickerton, S.; Babu, R. P.; Thayumanavan, S. *J. Am. Chem. Soc.* **2010**, *132*, 17227−17235. (c) Bickerton, S.; Jiwpanich, S.; Thayumanavan, S. *Mol. Pharmaceutics* **2012**, *9*, 3569−3578.
(35) Chen, K. J.; Chiu, Y. L.; Chen, Y. M.; Ho, Y. C.; Sung, H. W. *Biomaterials* **2011**, *32*, 2586−2592.
(36) Lu, J.; Owen, S. C.; Shoichet, M. S. *Macromolecules* **2011**, *44*, 6002−6008.
(37) Hua, P.; Tirelli, N. *React. Funct. Polym.* **2011**, *71*, 303−314.
(38) McDonald, T. O.; Martin, P.; Patterson, J. P.; Smith, D.; Giardiello, M.; Marcello, M.; See, V.; O'Reilly, R. K.; Owen, A.; Rannard, S. *Adv. Funct. Mater.* **2012**, *22*, 2469−2478.
(39) (a) Li, Y. P.; Budamagunta, M. S.; Luo, J. T.; Xiao, W. W.; Voss, J. C.; Lam, K. S. *ACS Nano* **2012**, *6*, 9485−9495. (b) Li, Y. P.; Xiao, W. W.; Xiao, K.; Berti, L.; Luo, J. T.; Tseng, H. P.; Fung, G.; Lam, K. S. *Angew. Chem., Int. Ed.* **2012**, *51*, 2864−2869.
(40) Javali, N. M.; Raj, A.; Saraf, P.; Li, X.; Jasti, B. *Pharm. Res.* **2012**, *29*, 3347−3361.
(41) Klymchenko, A. S.; Roger, E.; Anton, N.; Anton, H.; Shulov, I.; Vermot, J.; Mely, Y.; Vandamme, T. F. *RSC Adv.* **2012**, *2*, 11876−11886.
(42) The ^{1}H NMR spectrum (400 MHz, $CDCl_3$) of **3** indicates the ratio between the hydrophobic and hydrophilic segments to be 2.5. This value was estimated from the integrals of the resonances associated with the methyl protons at the termini of the decyl and oligo(ethylene glycol) chains.
(43) The amphiphilic character of the polymer controls its ability to form nanostructured particles. As a result, the ratio between its hydrophilic and hydrophobic segments (see ref 42) can presumably affect the hydrodynamic diameter of the nanoparticles as well as the critical polymer concentration required for their assembly.
(44) The overlap integral (J) and Förster distance (R_0) were calculated with eqs 1 and 2, respectively (Lakowicz, J. R. *Principles of Fluorescence Spectroscopy*; Springer: New York, 2006). The emission intensity (I_D) of the anthracene donor and the molar extinction coefficient (ε_A) of the BODIPY acceptor at a given wavelength (λ) were determined from the corresponding emission and absorption spectra (***c*** and ***b*** in Figure 1), respectively. The orientation factor (κ^2), fluorescence quantum yield (ϕ_D) of the donor, and refractive index (n) of the solvent are 2/3, 0.61, and 1.33 respectively.

$$J = \frac{\int_0^\infty I_D \varepsilon_A \lambda^4 d\lambda}{\int_0^\infty I_D d\lambda} \quad (1)$$

$$R_0 = \sqrt[6]{\frac{9000(\ln 10)\kappa^2 \phi_D J}{128\pi^5 N n^4}} \quad (2)$$

.
(45) Fluorescence images (***a***−***c*** in Supplementary Figure S5) recorded after incubation of the cells with the two sets of nanoparticles and Hoechst 33342 clearly show that the nanocarriers do not co-localize with this particular dye in the nucleus.
(46) The emission intensities of the bars in Figure 4 are reported relative to that of an indocyanine green standard. This compound was added to the cells 30 min prior to termination of incubation with the nanoparticles, and its fluorescence was recorded between 780 and 800 nm with excitation at 628 nm. The corresponding images are reported in the Supporting Information (***a***−***d*** in Figures S6−S8).
(47) Sahay, G.; Batrakova, E. V.; Kabanov, A. V. *Bioconjugate Chem.* **2008**, *19*, 2023−2029.
(48) Sakai-Kato, K.; Un, K.; Nanjo, K.; Nishiyama, N.; Kusuhara, H.; Kataoka, K.; Kawanishi, T.; Goda, Y.; Okud, H. *Biomaterials* **2014**, *35*, 1347−1358.
(49) Rejman, J.; Bragonzi, A.; Conese, M. *Mol. Ther.* **2005**, *12*, 468−474.
(50) Gabe, Y.; Urano, Y.; Kikuchi, K.; Kojima, H.; Nagano, T. *J. Am. Chem. Soc.* **2004**, *126*, 3357−3367.
(51) Lakowicz, J. R. *Principles of Fluorescence Spectroscopy*; Springer: New York, 2006.